

## Synthesis, Characterization, and Inelastic Neutron Scattering Study of Hydrogen Insertion Compounds of VO<sub>2</sub>(Rutile)

A. M. CHIPPINDALE,\* P. G. DICKENS, AND A. V. POWELL

*Inorganic Chemistry Laboratory, South Parks Road, Oxford OX1 3QR,  
United Kingdom*

Received November 27, 1990

Hydrogen insertion compounds, H<sub>x</sub>VO<sub>2</sub> (rutile) (0 < x < 0.37), have been prepared at ambient temperatures both chemically, by hydrogen spillover, and electrochemically, with subsequent characterization by powder X-ray diffraction and chemical analysis. For H<sub>x</sub>VO<sub>2</sub> (0.16 < x < 0.37), distortion of the monoclinic parent oxide occurs to give an orthorhombic rutile-related structure with lattice parameters similar to those of VO<sub>2-x</sub>(OH)<sub>x</sub> formed by the high-pressure, high-temperature decomposition of ammonium metavanadate, reported previously. The vibrational spectrum of H<sub>0.3</sub>VO<sub>2</sub> has been measured using inelastic neutron scattering spectroscopy. The spectrum and the corresponding vibrational analysis further confirm that the hydrogen insertion compound can be formulated as an oxyhydroxide. © 1991 Academic Press, Inc.

### Introduction

Vanadium dioxide exists as a number of polymorphs; three of which, VO<sub>2</sub> (rutile) (1), VO<sub>2</sub> (A) (2), and VO<sub>2</sub> (B) (3), have been well characterized. The most stable form, VO<sub>2</sub> (rutile), has the ideal tetragonal rutile structure at temperatures above 340 K and exhibits metallic conductivity. Below this temperature, however, it distorts to a semiconducting monoclinic form which contains V-V pairs. To date, compounds of the form H<sub>x</sub>VO<sub>2</sub> (0 < x < 1) with rutile-related structures have been prepared only under high-temperature and/or high-pressure conditions. For example, one polymorph of stoichiometric VOOH, which is isostructural with InOOH and β-CrOOH, can be prepared hydrothermally

from V<sub>2</sub>O<sub>3</sub> at 80 kbar and 873 K (4). A second polymorph, which has the diaspore (α-AlOOH) structure, in which double rutile chains share vertices, occurs naturally as the mineral montroseite and can also be synthesized under hydrothermal conditions by hydrolysis of NaVO<sub>3</sub> previously reduced under hydrogen (5). More recently, a nonstoichiometric phase, VO<sub>2-x</sub>(OH)<sub>x</sub> (0.13 < x < 0.37), with the CaCl<sub>2</sub>-distorted variant of the rutile structure, has been reported by Range and Zintl as one of the products of high-pressure, high-temperature decomposition of ammonium metavanadate at >20 kbar and 973-1073 K (6, 7).

In the present work, we describe the ambient-temperature synthesis, characterization, and inelastic neutron scattering spectrum of hydrogen insertion compounds of VO<sub>2</sub> (rutile), H<sub>x</sub>VO<sub>2</sub> (0 < x < 0.37).

\* To whom correspondence should be addressed.

## I. Preparation and Characterization of H<sub>x</sub>VO<sub>2</sub>

### (i) Preparation and Characterization of VO<sub>2</sub>

Powder X-ray diffraction data, recorded using a Stöe–Guinier focusing camera with CuK $\alpha$  radiation ( $\lambda = 1.54178 \text{ \AA}$ ), were used both for phase identification and as an indication of the purity of all the compounds prepared. The mean oxidation state of vanadium in each sample was determined by the reducing-power method of Choain and Marion (8). The parent oxide VO<sub>2</sub> was prepared by heating a stoichiometric mixture of V<sub>2</sub>O<sub>5</sub> and V<sub>2</sub>O<sub>3</sub> in an evacuated silica tube at 1173 K for 1 week. Reducing-power analysis gave the composition as VO<sub>2.01 $\pm$ 0.01</sub>, and comparison of the X-ray data with those of Longo and Kierkegaard (9) further confirmed that the product was monoclinic VO<sub>2</sub>.

### (ii) Preparation of H<sub>x</sub>VO<sub>2</sub> by Hydrogen Spillover

A series of hydrogen insertion compounds, H<sub>x</sub>VO<sub>2</sub>, was prepared by hydrogen spillover at room temperature and at 365 K using a finely dispersed platinum catalyst as described previously (10, 11). The uptake of hydrogen at room temperature was extremely slow and the maximum composition achieved was H<sub>0.08 $\pm$ 0.02</sub>VO<sub>2</sub>. The powder X-ray diffraction pattern of this product closely resembled that of the parent oxide. The hydrogen insertion reaction proceeded much more rapidly at 363 K and the maximum composition obtained at this temperature was H<sub>0.37 $\pm$ 0.01</sub>VO<sub>2</sub>. The product was shown to be inhomogeneous as the X-ray diffraction pattern contained two series of lines, one of which could be indexed on the basis of the monoclinic VO<sub>2</sub> unit cell and the other on a VO<sub>2</sub>-related orthorhombic unit cell. Heating the sample at 423 K in an evacuated, sealed Pyrex tube for 2 months produced a homogenous, monophasic product, with X-ray lines indexable on the ortho-

TABLE I  
POWDER X-RAY DATA FOR H<sub>0.37</sub>VO<sub>2</sub>

Intensity	2 $\theta$	$d_{\text{obs}}$ (Å)	$d_{\text{calc}}$ (Å)	$h$	$k$	$l$
s	27.379	3.257	3.254	1	1	0
m	36.475	2.463	2.460	0	1	1
m	37.001	2.429	2.428	1	0	1
vw	38.178	2.357	2.356	0	2	0
m	41.837	2.159	2.158	1	1	1
w	43.340	2.088	2.087	1	2	0
vwv	44.636	2.030	2.031	2	1	0
mw	54.240	1.691	1.691	1	2	1
m	55.392	1.659	1.660	2	1	1
mw	56.595	1.626	1.627	2	2	0
wm	64.663	1.441	1.442	0	0	2
w	67.946	1.380	1.379	0	3	1
w	70.978	1.328	1.330	3	0	1
w	71.579	1.318	1.318	1	1	2

Note. Refined orthorhombic lattice parameters (Å):  $a = 4.499(1)$ ,  $b = 4.712(1)$ , and  $c = 2.883(1)$ ; cf. VO<sub>1.63</sub>(OH)<sub>0.37</sub>(6):  $a = 4.502$ ,  $b = 4.649$ ,  $c = 2.870 \text{ \AA}$ .

rhombic unit cell alone (Table I). Two further single-phase compounds, H<sub>x</sub>VO<sub>2</sub> of intermediate composition ( $x = 0.16, 0.30$ ), were also prepared by spillover at 363 K, followed by several weeks' equilibration. These also show an orthorhombic distortion and their lattice parameters are given in Table II. The three high-hydrogen-content compounds were not air-sensitive; their reducing power remained constant over a number of months. However, the low-hydrogen-content phase was readily oxidized in air to VO<sub>2</sub>.

Two phases of H<sub>x</sub>VO<sub>2</sub> can thus be identified from their powder X-ray diffraction patterns. For small values of  $x$  ( $0 < x < 0.08$ ), H<sub>x</sub>VO<sub>2</sub> retains the monoclinic VO<sub>2</sub> (rutile) structure, while over the composition range ( $0.16 < x < 0.37$ ), distortion of the rutile-type structure occurs to give an orthorhombic unit cell. The orthorhombic distortion appears as a splitting of the ( $hkl$ ) reflections with  $h \neq k$ , and the extent of the splitting increases with increasing hydrogen content. The lattice parameters of this phase are in close agreement with those

TABLE II  
LATTICE PARAMETERS FOR  $H_xVO_2$

$x$	Structure type	$a$ (Å)	$b$ (Å)	$c$ (Å)	
0.0	VO <sub>2</sub> tetragonal <sup>a</sup>	4.554	4.554	2.847	
0.08	VO <sub>2</sub> monoclinic	5.759(3)	4.533(3)	5.372(3)	122.49(1)
0.16	Orthorhombic	4.525(2)	4.609(2)	2.863(3)	
0.30	Orthorhombic	4.505(3)	4.633(4)	2.869(1)	
0.37	Orthorhombic	4.499(1)	4.712(1)	2.883(2)	
1.00	Orthorhombic	4.446	4.862	2.962	(4)

<sup>a</sup> Extrapolated values for tetragonal lattice parameters at 298 K (6).

of VO<sub>2-x</sub>(OH)<sub>x</sub> (0.13 <  $x$  < 0.37) prepared by Range and Zintl (6) by the high-pressure, high-temperature decomposition of ammonium metavanadate.

### (iii) Electrochemistry

The electrochemical behavior of VO<sub>2</sub> in acidic media was also investigated. VO<sub>2</sub> was intimately mixed with PTFE and graphite (~10% by weight each) and pressed onto a platinum grid to form the cathode of a conventional three-compartment cell (12). Platinum foil was used as the anode, and the reference electrode was a saturated calomel electrode. A Princeton constant-current controller was used to monitor the galvanostatic discharge curves.

In conventional aqueous acid electrolytes such as 0.05 M H<sub>2</sub>SO<sub>4</sub>, VO<sub>2</sub> proved to be a very unstable cathode material as both the parent oxide and the insertion products dissolved before the discharge was complete. However, a galvanostatic discharge curve was obtained at 298 K under nonaqueous conditions, using an electrolyte of deoxygenated 0.099 M toluene(IV) sulphonic acid monohydrate in dry EtOH (13) at a current of 5  $\mu$ A (Fig. 1). The initial voltage (vs the standard hydrogen electrode) was 630 mV with a small plateau at 220 mV (0.02  $\leq x$  < 0.04). Hydrogen insertion proceeded only to a value of  $x = 0.06$  before the voltage fell to zero. This is in reasonable agreement

with the maximum value of  $x = 0.08$  achieved by hydrogen spillover at room temperature. Similar behavior was observed for the insertion of hydrogen into CrO<sub>2</sub> (14). The maximum achieved electrochemically at room temperature is H<sub>0.1</sub>CrO<sub>2</sub>, which retains the rutile structure, while spillover at 423 K gives orthorhombic H<sub>0.8</sub>CrO<sub>2</sub> (14).

## II. Vibrational Study of H<sub>0.3</sub>VO<sub>2</sub>

### (i) Inelastic Neutron Scattering Spectrum of H<sub>0.3</sub>VO<sub>2</sub>

The metallic nature of H<sub>x</sub>VO<sub>2</sub> makes optical spectroscopic measurements difficult. The vibrational spectrum was therefore measured using inelastic neutron scattering (INS) spectroscopy. This technique has proved useful in the past for investigating the nature of the hydrogen attachment in insertion compounds, e.g., H<sub>x</sub>WO<sub>3</sub> (15), H<sub>x</sub>MoO<sub>3</sub> (16), and H<sub>x</sub>V<sub>2</sub>O<sub>5</sub> (17), since the large incoherent scattering cross section of hydrogen results in their INS spectra being dominated by vibrational modes involving hydrogen displacements.

The spectrum of H<sub>0.3</sub>VO<sub>2</sub> was recorded at 80 K over the range 250–2000 cm<sup>-1</sup> using the IN1 BeF spectrometer at the ILL, Grenoble. Nine grams of H<sub>0.3</sub>VO<sub>2</sub>, prepared by hydrogen spillover and characterized as above, was loaded under nitrogen into a

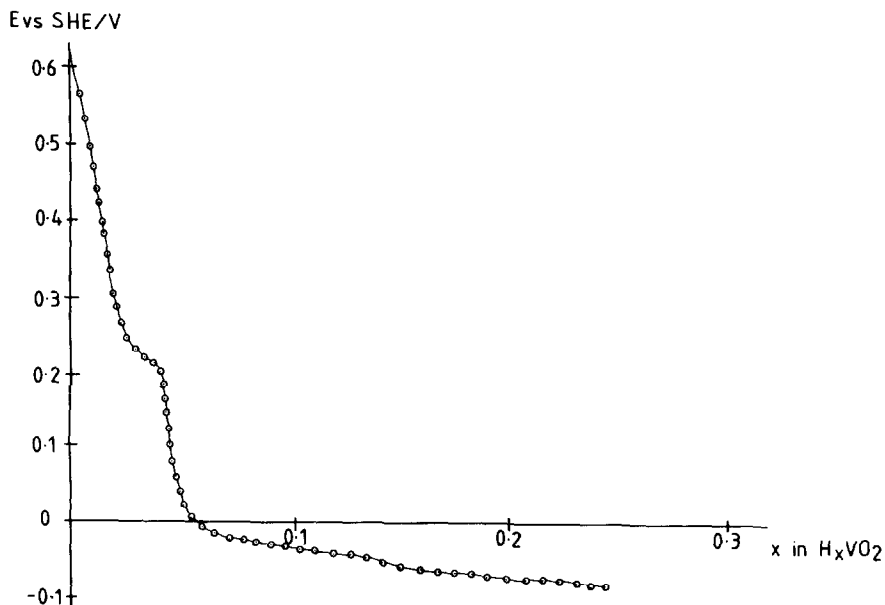


FIG. 1. Galvanostatic discharge curve of H<sub>x</sub>VO<sub>2</sub> at 5 μA in 0.1 M toluene(IV) sulphonic acid at 298 K.

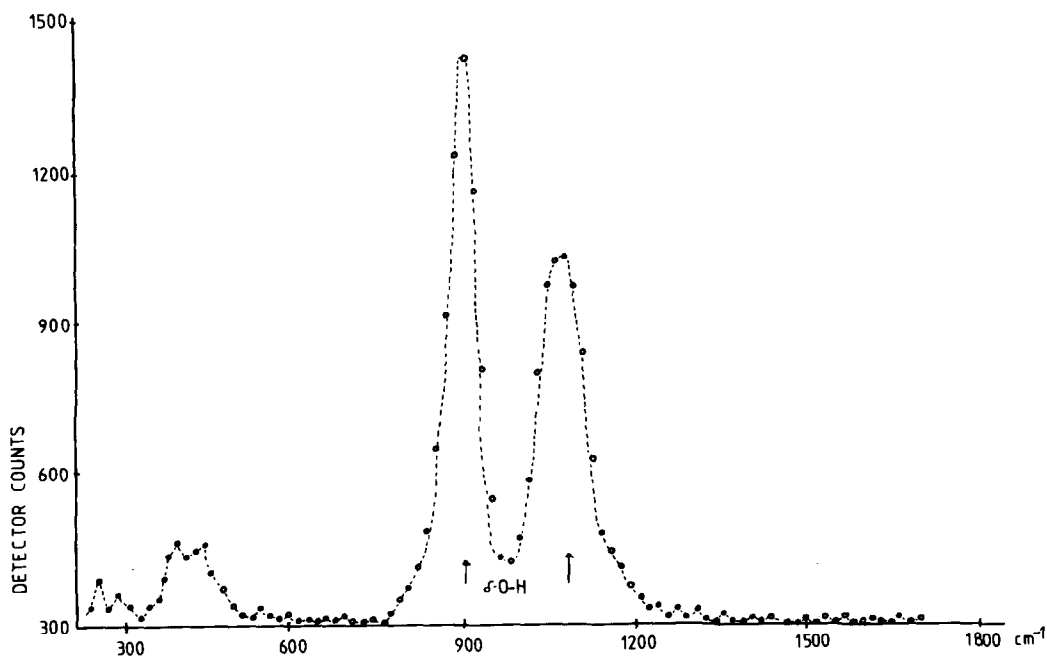


FIG. 2. Inelastic neutron scattering spectrum of H<sub>0.3</sub>VO<sub>2</sub> at 80 K.

TABLE III  
ATOM PARAMETERS FOR  $H_4V_2O_4$

	$x/a$	$y/b$	$z/c$
V	0	0	0
O	0.286	0.312	0
H <sup>b</sup>	0.1202	0.433	0

<sup>a</sup> No provision for partial occupancy of sites can be made in this program, and H's accordingly are placed on all 4(*g*) sites.

<sup>b</sup> H atoms were not located in (*6*) and by analogy with the isostructural  $\beta$ -HCrO<sub>2</sub> (19), H atoms are placed at 1 Å from the nearest O atom.

number of high-purity silica tubes (approximately 3-mm internal diameter) to a depth of 5 cm. The tubes were evacuated and sealed. They were then arranged in a drilled aluminium block, designed to present the maximum sample volume to the neutron beam, mounted on a sample stick, and loaded into an ILL orange cryostat on the sample table. Previous experiments have shown that the scattering from the silica tubes produces little contribution to the background spectrum and can be ignored (15).

The INS spectrum of  $H_{0.3}VO_2$  shows two intense peaks at 1083 and 909  $\text{cm}^{-1}$  and two smaller ones at 476 and 431  $\text{cm}^{-1}$ . (Fig. 2). Assignment to vibrational modes is discussed below.

### (ii) Calculation of the Vibrational Spectrum of $H_{0.3}VO_2$

Fundamental vibrational frequencies and corresponding atomic displacements were calculated using the program SOTONVIB (18). A simple valence force field (SVFF),

$$2V = \sum_i k_{r_i} \Delta r_i^2 + \sum_j k_{\theta_j} \Delta \theta_j^2,$$

involving bond stretches,  $\Delta r_i$  and angle deformation,  $\Delta \theta_j$  was chosen. The SOTONVIB input requirement is for atomic masses, Cartesian coordinates of all atoms in the unit cell, definition of enough internal coordinates to cover all vibrational degrees of freedom, and chosen values for the force constants  $k_{r_i}$  and  $k_{\theta_j}$ . The complete input file used for this purpose may be obtained on request to the authors; essential data involved are summarized in Table III.

*Atomic parameters.* A plan of the unit cell is shown in Fig. 3; also shown are the positions of neighboring atoms needed to complete the specification of all the internal coordinates used, which are based on changes in V–O and O–H bond lengths and VOV, OVO, and VOH bond angles.

*Force constants.* V–O stretching force constants were chosen by scaling, according to length, the force constants of the V–O stretch in the  $V_3O$  unit in  $V_2O_5$  (20). The VOV and OVO deformation force constants were taken to be the same as those of the corresponding bends in the  $V_3O$  unit of  $V_2O_5$ . The remaining force constants were chosen to fall within the range of previously published values for similar motions. Chosen values are given in Table IV (with atom numbering as in Fig. 3).

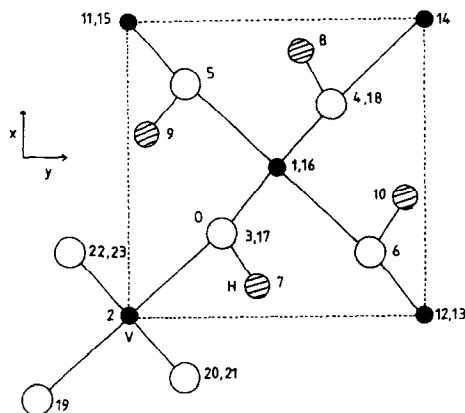


FIG. 3. Unit cell of  $H_4V_2O_4$ .

TABLE IV  
 FORCE CONSTANTS FOR H<sub>4</sub>V<sub>2</sub>O<sub>4</sub>

Bond stretch	$k_r$ (mdyn Å <sup>-1</sup> )	Angle bend	$k_\theta$ (mdyn Å rad <sup>-2</sup> )
V(1)-O(4)	1.14	VOV(all)	0.23
V(1)-O(5)	1.14	OVO(all)	0.30
O-H	6.43	V(1)O(6)H(10)	0.35
		V(1)O(3)H(7)	0.40

*Calculated vibrations.* For H<sub>4</sub>V<sub>2</sub>O<sub>5</sub>, 27 optic modes are predicted belonging to the representation

$$4A_g + 4B_{1g} + 2B_{2g} + 2B_{3g} + 3A_u + 2B_{1u} + 5B_{2u} + 5B_{3u}.$$

The calculated frequencies and their assignments (based on calculated atomic displacements) are shown in Table V.

The main features of the calculated modes can be shown by a consideration of the atomic displacements about one of the four V<sub>3</sub>OH units (Fig. 4). The O-H stretch calculated at approximately 3400 cm<sup>-1</sup> lies outside the range of the IN1 spectrometer. The two main peaks found in the measured spectrum at 1083 and 909 cm<sup>-1</sup> coincide nicely with the calculated orthogonal δ-VOH bend-

ing modes (one set in the *xy* plane, the other in the *z* direction). The high intensities observed for these peaks in the spectrum of H<sub>0.3</sub>VO<sub>2</sub> confirm that they correspond to modes involving large hydrogen displacements. The vibrations, calculated at approximately 580 cm<sup>-1</sup> and below, involve principally V-O stretching and bending modes which carry hydrogen along with the oxygen displacement and this accounts for their prominent appearance in the INS spectrum. The assignments made at 476 and 431 cm<sup>-1</sup> agree well with Beattie's previous analysis of the motions of almost-planar M<sub>3</sub>O units in compounds such as V<sub>2</sub>O<sub>5</sub>, MoO<sub>3</sub>, and TiO<sub>2</sub> (rutile and anatase) where in-plane modes occur in the region 830-470 cm<sup>-1</sup> and out-of-plane modes in the region 360-120 cm<sup>-1</sup> (21).

Use of a more sophisticated force field would allow greater "fine-tuning" to measured frequencies but the present analysis serves to account for most of the main features of the observed spectrum. The marked splitting observed for the δM-OH vibration here is also found for a number of other oxyhydroxides containing M<sub>3</sub>OH groups such as α-AlO(OH) (diaspore) (22), GaO(OH) (23), and β-CrO(OH) (24). In the last example, the bending modes, observed

 TABLE V  
 FREQUENCIES AND ASSIGNMENTS OF GENERATED VIBRATIONAL MODES OF H<sub>4</sub>VO<sub>2</sub>

Calculated frequency (cm <sup>-1</sup> )	Observed frequency (cm <sup>-1</sup> )	Assignment	Mode
3407 (× 4)		B <sub>1g</sub> B <sub>3u</sub> B <sub>2u</sub> A <sub>g</sub>	ν(O-H)
1098 1095	1083	B <sub>2u</sub> B <sub>3u</sub> B <sub>1g</sub> A <sub>g</sub>	δ(O-H) in <i>xy</i> plane
1093 1092			
918 916 914	909	B <sub>1u</sub> A <sub>u</sub> B <sub>3g</sub> B <sub>2g</sub>	δ(O-H) out of <i>xy</i> plane
914			
587 583 553	476 431	B <sub>3u</sub> B <sub>2u</sub> B <sub>1u</sub> A <sub>g</sub>	Lattice modes
517 515 493		B <sub>1g</sub> A <sub>u</sub> B <sub>3g</sub> B <sub>2g</sub>	
414 414 342		B <sub>2u</sub> B <sub>1g</sub> B <sub>3u</sub>	
342 341 322		B <sub>3u</sub> B <sub>2u</sub> A <sub>u</sub> A <sub>g</sub>	
292 267 212			
177			

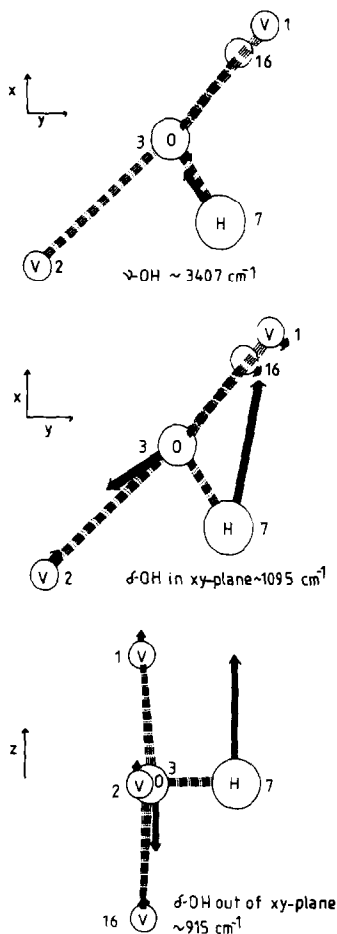


FIG. 4. Generated atomic displacements of  $V_3OH$  unit.

in both IR and INS spectra (24), occur at higher frequencies than in  $H_{0.3}VO_2$ , i.e., at 1391 and  $1215 \text{ cm}^{-1}$ , reflecting the greater strength of hydrogen bonding in this compound. The O–O distance is  $2.46 \text{ \AA}$  in  $\beta\text{-CrCr(OH)}$  compared with  $3.11 \text{ \AA}$  in  $VO_{1.7}(OH)_{0.3}$  (6).

### III. Conclusions

Two phases of  $H_xVO_2$  ( $0 < x < 0.37$ ) have been prepared and characterized. The low-hydrogen-content phase ( $0 < x < 0.08$ ), prepared at room temperature electrochemi-

cally and by hydrogen spillover, is monoclinic and has lattice parameters little changed from those of the parent oxide  $VO_2$ . The small tunnels in the  $VO_2$  structure and the highly crystalline nature of the oxide, which was prepared at a high temperature, may restrict the mobility of the hydrogen through the bulk of the solid. Structural distortions occur upon the formation of the higher-hydrogen-content phase of  $H_xVO_2$  ( $0.16 < x < 0.37$ ) and this is only readily achieved by spillover at temperatures above the  $VO_2$  monoclinic–tetragonal transition temperature.  $H_xVO_2$  ( $0.16 < x < 0.37$ ) is orthorhombic and has been shown by INS to contain  $-OH$  groups. It is thus clearly identifiable with  $VO_{2-x}(OH)_x$  ( $0.13 < x < 0.37$ ) prepared previously by high-temperature–high-pressure decomposition of ammonium metavanadate (6). Thus, what was formerly regarded as a high-pressure phase of  $H_xVO_2$  has been prepared under ambient conditions in the present investigations by the reaction of  $VO_2$  and atomic hydrogen.

### Acknowledgments

The authors thank Professor I. R. Beattie, University of Southampton, for making available the program "SOTONVIB." In addition, AVP thanks the CEGB for financial support and AMC thanks New College, Oxford, for a research fellowship.

### References

1. G. ANDERSSON, *Acta Chem. Scand.* **10**, 623 (1956).
2. Y. OKA, T. YAO, AND N. YAMAMOTO, *J. Solid State Chem.* **86**, 116 (1990).
3. F. THEOBALD, R. CABALA, AND J. BERNARD, *J. Solid State Chem.* **17**, 431 (1976).
4. J. CHENAVAS, J. C. JOUBERT, J. J. CAPPONI, AND M. MAREZIO, *J. Solid State Chem.* **6**, 1 (1973).
5. J. MULLER AND J. C. JOUBERT, *J. Solid State Chem.* **11**, 79 (1974).
6. K.-J. RANGE AND R. ZINTL, *Mater. Res. Bull.* **18**, 411 (1983).
7. K.-J. RANGE AND R. ZINTL, *Z. Naturforsch. B* **43**, 309 (1988).
8. C. CHOAIN AND F. MARION, *Bull. Soc. Chim. Fr.*, 212 (1963).
9. J. M. LONGO AND P. KIERKEGAARD, *Acta Chem. Scand.* **24**, 420 (1970).

10. G. C. BOND AND P. A. SERMON, *Catal. Rev.* **8**, 211 (1973).
11. P. A. SERMON AND G. C. BOND, *J. Chem. Soc. Faraday Trans. 1* **72**, 730 (1976).
12. D. T. SAWYER AND J. L. ROBERTS, in "Experimental Electrochemistry for Chemists," Chap. 3, Wiley, New York (1974).
13. A. M. CHIPPINDALE, D. Phil. thesis, Oxford (1987).
14. M. T. WELLER, Chemistry Part II thesis, Oxford (1982).
15. C. J. WRIGHT, *J. Solid State Chem.* **20**, 89 (1977).
16. P. G. DICKENS, J. J. BIRTILL, AND C. J. WRIGHT, *J. Solid State Chem.* **28**, 185 (1979).
17. G. C. BOND, P. A. SERMON, AND C. J. WRIGHT, *Mater. Res. Bull.* **19**, 701 (1984).
18. I. R. BEATTIE, N. CHEETHAM, M. GARDNER, AND D. E. ROGERS, *J. Chem. Soc. A*, 2240 (1971).
19. A. N. CHRISTENSEN, P. HANSEN, AND M. S. LEHMANN, *J. Solid State Chem.* **19**, 299 (1976).
20. T. R. GILSON, O. F. BIZRI, AND N. CHEETHAM, *J. Chem. Soc. Dalton Trans.*, 291 (1973).
21. I. R. BEATTIE AND T. R. GILSON, *J. Chem. Soc. A*, 2322 (1969).
22. E. HARTERT AND O. GLEMSE, *Z. Elektrochem.* **60**, 746 (1956).
23. M. F. PYE, Chemistry Part II thesis, Oxford (1975).
24. M. T. WELLER, D. Phil. thesis, Oxford (1984).